
On catastrophic forgetting and mode collapse in Generative Adversarial Networks

Hoang Thanh-Tung¹ Truyen Tran¹ Svetha Venkatesh¹

Abstract

Generative Adversarial Networks (GAN) (Goodfellow et al., 2014) are one of the most prominent tools for learning complicated distributions. However, problems such as mode collapse and catastrophic forgetting, prevent GAN from learning the target distribution. These problems are usually studied independently from each other. In this paper, we show that both problems are present in GAN and their combined effect makes the training of GAN unstable. We also show that methods such as gradient penalties and momentum based optimizers can improve the stability of GAN by effectively preventing these problems from happening. Finally, we study a mechanism for mode collapse to occur and propagate in feedforward neural networks.

1. Introduction

Generative Adversarial Networks (Goodfellow et al., 2014) are one of the most common tools for learning complex distributions. GAN learn to generate samples from a target distribution p_x by playing a competitive game between two players: the generator G and the discriminator D . At every iteration of the game, the generator transforms a noise vector $z \sim p_z$ to a vector $\tilde{x} = G(z)$ that is similar to samples from the target distribution p_x . The discriminator tries to separate fake samples \tilde{x} from real samples $x \sim p_x$.

GAN are known for their capability to produce realistic samples. However, the original GAN is tricky to train and often suffer from problems such as mode collapse and catastrophic forgetting. Mode collapse is the problem where G maps different inputs $z^{(1)}$ and $z^{(2)}$ to the same output \tilde{x} . Catastrophic forgetting in neural networks (French, 1999) is the phenomenon where the learning of new skill catastrophically damage the performance of the previously learned

¹Deakin University. Correspondence to: Hoang Thanh-Tung <hoangtha@deakin.edu.au>.

skills. In machine learning literatures, mode collapse and catastrophic forgetting are usually studied independently. A number of methods have been proposed to address mode collapse (Radford et al., 2015; Arjovsky et al., 2017) and catastrophic forgetting (Kirkpatrick et al., 2017; Shin et al., 2017; Zenke et al., 2017) as independent problems.

In this paper, we show that catastrophic forgetting is present in GAN and it could combine with mode collapse to make the training even more unstable. We demonstrate scenarios where the combined effect of catastrophic forgetting and mode collapse causes the generator and the discriminator to fall into a learning loop. We then study methods for alleviating these problem. Our results show that gradient penalties (Gulrajani et al., 2017; Kodali et al., 2017) and momentum based optimizers (Qian, 1999) help the discriminator to distribute its capacity more equally between different regions of the data manifold and between different time steps. Gradient penalties also spread fake samples over the real data manifold, effectively helping GAN to avoid mode collapse.

Our contributions are as follow:

1. We study the effect of catastrophic forgetting in GAN. We show how catastrophic forgetting could lead to unstable training.
2. We explain how methods for stabilizing GAN such as gradient penalties and momentum based optimizers can help to prevent catastrophic forgetting and mode collapse in GAN.
3. We study the formation and the propagation dynamic of mode collapse in feedforward neural networks.

2. Catastrophic forgetting in GAN

In GAN, there are a number of scenarios where catastrophic forgetting can hurt the generative performance:

1. GAN are used to learn a set of distributions p_r^0, \dots, p_r^N that are introduced sequentially.
2. GAN are used to a single distribution p_r .

The first scenario is standard in continual learning. The

discriminator D at task n does not have access to distributions p_r^0, \dots, p_r^{n-1} . D , thus, forgets about previous real distributions and cannot teach the generator G to generate samples from these distributions. In order to maximally deceive D , G only produces samples from p_r^n . A number of methods (Kirkpatrick et al., 2017; Shin et al., 2017; Zenke et al., 2017) have been proposed to address catastrophic forgetting in this setting. Seff et al. (2017) used Elastic Weight Consolidation (EWC) algorithm in Kirkpatrick et al. (2017) to solve catastrophic forgetting in GAN in this setting and achieved promising results.

The second scenario is the subject of this section. It can also be viewed as a continual learning problem in which D has to discriminate a sequence of model distributions p_G^0, \dots, p_G^T , (where T is the number of training iterations) from the target distribution p_r , and G has to deceive a sequence of discriminators D^0, \dots, D^T . At step t , D still has access to samples from the target distribution p_r , but it cannot access to samples from previous model distributions $p_G^i, i = 0 : t-1$. As a result, D is biased toward discriminating the current model distribution p_G^t from the target distribution, forgetting previous model distributions. Furthermore, D focuses on separating fake samples from nearby real samples, ignoring distant real samples.

In Fig. 1, the gradient points in the direction that increases the score $D(\mathbf{x})$ so data points on the left of the green box have higher scores than points on the right. D assigns higher score to data points that are further away from fake samples, regardless of the true label of these points. It is interesting to note that data points on the right of the red box in Fig. 1a have higher score than real data points located around coordinates (1.0, 1.0) and (0.0, 1.5). Furthermore, gradients w.r.t. data points that D has forgotten point in wrong directions (red box in Fig. 1a) or have small norms (blue boxes in Fig. 1a). That implies that D overemphasizes on the current fake samples and nearby real samples while lowering the importance of distant real samples. In other words, the performance of D on old and distant samples is catastrophically damaged by the learning of the current task. We note that distant real samples are present in every mini-batch as we used large mini-batches of size from 32 to 256 in our experiments. Catastrophic forgetting happens not only because the data of old tasks are no longer accessible, but also because of the way the network distribute its capacity.

If G has mode collapse, then D only focuses on a small set of modes of p_r that are close to samples produced by G , and forgets about other modes. That worsens catastrophic forgetting in D , making D unable to guide G to other modes of p_r . G also has the chance to fool D by reintroducing samples from previous iterations. When this situation occurs, D and G could fall into a loop and will not settle at an equilibrium. For the experiment in Fig. 1, the loop continues for many

cycles without any sign of breaking.

Formulating GAN learning as a continual learning problem allows us to borrow methods from continual learning literature to improve the stability of GAN. In the next subsections, we discuss how recently developed methods for stabilizing GAN can help to prevent both mode collapse and catastrophic forgetting.

2.1. Gradient penalties

When D forgets a distant data point, the negative gradient $-\frac{\partial \mathcal{L}_D}{\partial \mathbf{x}}$ has small norm (blue box in Fig. 1a) and/or points in wrong direction (green box in Fig. 1a). We can prevent D from forgetting distant real data point \mathbf{x} by forcing the norm of negative gradients with respect to data points around \mathbf{x} to be large and point toward \mathbf{x} . This could be achieved by adding a gradient penalty term to the loss \mathcal{L}_D . Motivated by the properties of Wasserstein distance, Gulrajani et al. (2017) proposed a gradient penalty of the form:

$$\mathbb{E}_{\hat{\mathbf{x}}} \left[\left(\|\nabla_{\hat{\mathbf{x}}} D(\hat{\mathbf{x}})\|_2 - k \right)^2 \right] \quad (1)$$

where $\hat{\mathbf{x}} = \alpha \mathbf{x} + (1 - \alpha) \tilde{\mathbf{x}}$, $\alpha \sim U(0, 1)$, $\mathbf{x} \sim p_r$, $\tilde{\mathbf{x}} \sim p_G$ and $k = 1$.

Kodali et al. (2017) proposed to replace the interpolation with a point \mathbf{x}^* in the neighborhood of \mathbf{x} :

$$\mathbf{x}^* = \mathbf{x} + \epsilon$$

where $\epsilon \sim p_\epsilon$. In both versions, the negative gradient w.r.t a point $\hat{\mathbf{x}}$ in the neighborhood of \mathbf{x} has norm close to k . The risk of \mathbf{x} being forgotten is thus reduced.

We also note that if $k = 0$ then minimizing the expectation in equation 1 is equivalent to encouraging the gradient norm at every point to be equal (Cauchy-Schwarz inequality). As a result, the capacity of D is more equally distributed over different regions of the data space (Fig. 2c).

When the former gradient penalty is used, the score $D(\hat{\mathbf{x}})$ of a point $\hat{\mathbf{x}} = \alpha \mathbf{x} + (1 - \alpha) \tilde{\mathbf{x}}$ should increase as α increases. Therefore, the negative gradients along the line segment connecting $\tilde{\mathbf{x}}$ and \mathbf{x} are large and point toward \mathbf{x} (Fig. 2b illustrates the phenomenon on the toy dataset). As a result, $\tilde{\mathbf{x}}$ is attracted toward \mathbf{x} . When the expectation 1 is approximated using a mini-batch, different fake samples will be paired with different real samples. Different fake samples will thus be attracted toward different real samples. Different mini-batches of real samples move fake samples in different directions. That spreads fake samples over the real data manifold, effectively reduces mode collapse. Experiments in (Kodali et al., 2017; Fedus et al., 2018) verify that gradient penalty improves the diversity of generated samples.

Although this effect reduces mode collapse, it could make GAN not convergent. Because the pair $(\mathbf{x}, \tilde{\mathbf{x}})$ is chosen at

random, \tilde{x} will continually be attracted toward different real datapoints during training and will not converge to any real datapoint. A empirical way to fix this is to decay the weight of the gradient penalty term. Fig. 7 in the appendix shows that gradient penalty makes the training to oscillate.

Note that this does not contradict proposition 1 in Gulrajani et al. (2017). Proposition 1 states that gradient w.r.t. a point \hat{x} on the line segment connecting x and \tilde{x} has norm 1 if $(x, \tilde{x}) \sim \pi$, where π is the *optimal coupling between the real and the fake distribution*. For a fake datapoint \tilde{x} , the real datapoint x that \tilde{x} is coupled with is not chosen at random, but must follow an optimal strategy specified by π . In other words, \tilde{x} should not be attracted toward random real datapoints during training. However, finding the optimal coupling π is intractable, and Gulrajani et al. (2017) replaced it with the uniform joint distribution between real and fake samples.

When gradient penalty is not used, \tilde{x} is attracted toward its closest real data point x (Fig. 2a), regardless of which real samples are there in the mini-batch. This is because, unlike in gradient penalty, there is no connection between \tilde{x} and another real sample in the mini-batch. Consequently, the randomness in mini-batches cannot help \tilde{x} to escape the basin of attraction of x . If a large number of fake samples are attracted toward the same real sample, mode collapse happens. Fig. 2 demonstrates the effect of gradient penalty on a toy dataset.

2.2. Momentum based optimizers

In the experiment in Fig. 1, D assigns large gradients to points near the current fake and real samples, while assigning small gradients to distant real samples and old fake samples. The gradients also change their directions as rapidly as the fake samples move. Forgetting old gradient information makes the learning of D and therefore, G , slower and could cause learning loop. A solution is to remember gradient information for a longer period.

Momentum based optimizers (Qian, 1999) use the running average of the gradients for updating model’s parameters. SGD with momentum updates the model parameters as follows:

$$\mathbf{g}_t = \beta \mathbf{g}_{t-1} + (1 - \beta) \nabla_{\theta} f(\theta_{t-1}) \quad (2)$$

$$\theta_t = \theta_{t-1} - \alpha \mathbf{g}_t \quad (3)$$

The running average \mathbf{g}_t is a simple form of memory that accumulates gradient information from all previous steps. That helps the model to remember gradient information for a longer period and reduces the effect of catastrophic forgetting. The update in equation 3 will improve the performance of the model on samples in the current mini-batch and previous mini-batches. The direction of \mathbf{g}_t is less sensitive to

the current gradient $\nabla_{\theta} f(\theta_{t-1})$. Instead of focusing on the current mini-batch, the model distributes its capacity to many mini-batches. The model will thus generalize better. For the discriminator, it means that the discriminator can better differentiate fake samples from real samples from many different modes.

Fig. 3 shows how momentum based optimizers help to alleviate catastrophic forgetting in D . The figure shows the gradient w.r.t. the input of the discriminator $\frac{\partial \mathcal{L}_D}{\partial x}$, not the gradient w.r.t. the parameters $\frac{\partial \mathcal{L}_D}{\partial \theta}$. However, the stability in $\frac{\partial \mathcal{L}_D}{\partial x}$ implies the stability in $\frac{\partial \mathcal{L}_D}{\partial \theta}$.

We also note that although D can better remember its old gradients, it still cannot help G to escape from mode collapse. This is because the majority of G ’s outputs are concentrated in a small region of the space and are attracted toward the same real sample. In order to avoid mode collapse, we need to spread fake samples over a large region so that different fake samples are in the basin of attraction of different real samples. As discussed in previous subsection, gradient penalties are an effective tool for that. Batch normalization (Ioffe & Szegedy, 2015) keeps the variance of outputs at high values, also produces the effect of spreading fake samples over the space (see Fig. 5).

3. The formation and propagation of mode collapse

3.1. The relationship between weight matrix rank and mode collapse

Empirical studies found that multilayer perceptrons (MLPs) are very hard to train using original GAN loss (Goodfellow et al., 2014) while convolutional neural networks (CNNs) (LeCun et al., 1998; Fukushima, 1980) are more robust to mode collapse (Radford et al., 2015). We show here how the probability of mode collapse is related to the rank of weight matrices in FFNNs and that in turn, explains the robustness of CNNs.

Let us consider a L -layer MLP based generator that maps $z \in \mathbb{R}^d$ to $x \in \mathbb{R}^D$. Let $W^{(l)} \in \mathbb{R}^{m \times n}$, $m \geq n$, $\mathbf{b}^{(l)} \in \mathbb{R}^m$ be the weight matrix and bias at layer l ¹. If mode collapse happens at layer l , then for different input activations $\mathbf{a}^{(l,1)}, \mathbf{a}^{(l,2)} \in \mathbb{R}^n$

$$W^{(l)} \mathbf{a}^{(l,1)} + \mathbf{b}^{(l)} \approx W^{(l)} \mathbf{a}^{(l,2)} + \mathbf{b}^{(l)} \quad (4)$$

$$W^{(l)} (\mathbf{a}^{(l,1)} - \mathbf{a}^{(l,2)}) \approx \mathbf{0} \quad (5)$$

Mode collapse happens if $\mathbf{a}^{(l)} = \mathbf{a}^{(l,1)} - \mathbf{a}^{(l,2)}$ is in or close to the null space of $W^{(l)}$. The probability for a random vector $\mathbf{a}^{(l)}$ to fall in the null space of $W^{(l)}$ is higher when

¹ m is usually greater than n because generators map low dimensional noise to high dimensional output. The analysis here applies to the case where $n \geq m$ as well.

the dimensionality of the null space is higher or equivalently, the rank of $W^{(l)}$ is lower (the rank-nullity theorem).

If the input activations are random vectors in \mathbb{R}^n , then the outputs of this layer form a $k^{(l)}$ -dimensional manifold in \mathbb{R}^m , where $k^{(l)} = \text{rank}(W^{(l)}) \leq n$. The outputs of a low rank weight matrix are concentrated in a more compact region than the inputs². The inputs get more and more concentrated when passing through many layers with low rank weight matrices. When outputs are concentrated in a compact region, they are more likely to be attracted toward the same real data point, making mode collapse to happen.

The outputs of the generator are concentrated on a k -dimensional manifold in \mathbb{R}^D . If we assume that real data points are uniformly distributed in \mathbb{R}^D , then the number of real data points that the generator can approximate decreases exponentially with k . This is consistent with our observation that when mode collapse occurs, the number of significantly different samples that the generator can produce decrease exponentially fast.

As shown in 3.2, gradient descent tends to make W a low rank matrix. A fully connected layer has no mechanism to prevent gradient descent from decreasing the rank of its weight matrix.

A convolution operation that maps n dimensional inputs to m dimensional outputs can be converted to matrix multiplication with the weight matrix being a Toeplitz matrix W_{Toeplitz} . If at least one element of the kernel is non-zero, then the rank of W_{Toeplitz} is n . Therefore, the rank of the weight matrix in convolution operation is n for almost all of practical situations. The null space of W_{Toeplitz} contains a single vector $\mathbf{0} \in \mathbb{R}^n$. The outputs of the layer are scattered in a (at least) n dimensional subspace of \mathbb{R}^m and they are less likely to be attracted toward the same real sample. Consequently, mode collapse cannot happen in CNNs in the same way as in MLPs. Higher rank weight matrices and the large number of kernels make CNNs more robust to mode collapse than MLPs.

3.2. The propagation of mode collapse in MLPs

Let us consider a GAN as proposed in (Goodfellow et al., 2014) with discriminator D , generator G , and loss functions

$$\begin{aligned}\mathcal{L}_D &= \mathbb{E}_{\mathbf{x} \sim p_{\mathbf{x}}} [\log D(\mathbf{x})] + \mathbb{E}_{\mathbf{z} \sim p_{\mathbf{z}}} [\log(1 - D(G(\mathbf{z})))] \\ \mathcal{L}_G &= \mathbb{E}_{\mathbf{z} \sim p_{\mathbf{z}}} [-\log D(G(\mathbf{z}))]\end{aligned}$$

Let G be a MLP with ReLU activation function. Let $W = [\mathbf{x} \ \mathbf{y}] \in \mathbb{R}^{n \times 2}$ be G 's output layer's weight matrix. The bias

²Although activation functions can change the dimensionality of the manifold of outputs, they reduce the distance between outputs. This is because of the saturated regions in common activation functions such as *ReLU*, *tanh* and *sigmoid* map different inputs to (nearly) the same outputs.

is omitted for simplicity. Let $\mathbf{x}^*, \mathbf{y}^*$ be the real data points closest to \mathbf{x}, \mathbf{y} , respectively. We assume that \mathbf{x} is close to \mathbf{x}^* while \mathbf{y} is further away from \mathbf{y}^* :

$$\|\mathbf{y} - \mathbf{y}^*\| \gg \epsilon > \|\mathbf{x} - \mathbf{x}^*\|$$

where $\epsilon > 0$ is a small constant.

For a random input activation $\mathbf{a} \in \mathbb{R}^2$, the output is

$$\tilde{\mathbf{x}} = W\mathbf{a} = a_1\mathbf{x} + a_2\mathbf{y}$$

Because $\|\mathbf{y} - \mathbf{y}^*\| \gg \|\mathbf{x} - \mathbf{x}^*\|$, the closest real data point of $\tilde{\mathbf{x}}$ is more likely to be \mathbf{x}^* (see Fig. 4a). If $\tilde{\mathbf{x}}$ is in the basin of attraction of \mathbf{x}^* , then stochastic gradient descent update of G will move $\tilde{\mathbf{x}}$ toward \mathbf{x}^* .

More formally, if $\tilde{\mathbf{x}}$ is closer to \mathbf{x}^* , then the update according to the stochastic gradient $\frac{\partial \log(D(W\mathbf{a}))}{\partial W}$ will change W in a way that moves $W\mathbf{a}$ closer to \mathbf{x}^* . Because $\|\mathbf{x} - \mathbf{x}^*\|$ is already small, in order to move $W\mathbf{a}$ closer to \mathbf{x}^* , SGD update of W has to move \mathbf{y} closer to \mathbf{x}^* , effectively increases the cosine similarity measure between \mathbf{y} and \mathbf{x} (and between \mathbf{y} and \mathbf{x}^*). When \mathbf{y} is closer to \mathbf{x}^* , the probability that the output $\tilde{\mathbf{x}}$ is closer to \mathbf{x}^* increases (Fig. 4b). As the training continues, \mathbf{y} will get closer and closer to \mathbf{x}^* . More and more data points $\tilde{\mathbf{x}}$ will lie in the basin of attraction of \mathbf{x}^* . That causes mode collapse to happen.

In Fig. 4, when \mathbf{x} and \mathbf{y} become more similar, their conical combinations cover a smaller region of the space. The volume of the cone decreases exponentially fast as \mathbf{x} and \mathbf{y} become similar. If we assume that real data points are randomly distributed in \mathbb{R}^n , then when the columns of W become more similar, the number of real data points lie in the convex cone defined by the columns of W decreases exponentially.

Mode collapse propagates between columns of W . Because the loss \mathcal{L}_D does not penalize updates that make columns of W more similar, adding more columns to W cannot stop mode collapse from propagating. When mode collapse occurs, a large weight matrix cannot produce much more diverse samples than a small weight matrix.

For the same reason, adding more generators to the game also does not help to avoid mode collapse. However, a mixture of discriminators is better than a single discriminator at preventing mode collapse. Because of the randomness in mini-batches, different discriminators focus on different regions of the space. When they are used in training, they will move fake samples in different directions, helping to spread fake samples over the space. The effect is similar to that of gradient penalty. Arora et al. (2017) showed that using mixture of discriminators and mixture of generators improves the stability of GAN.

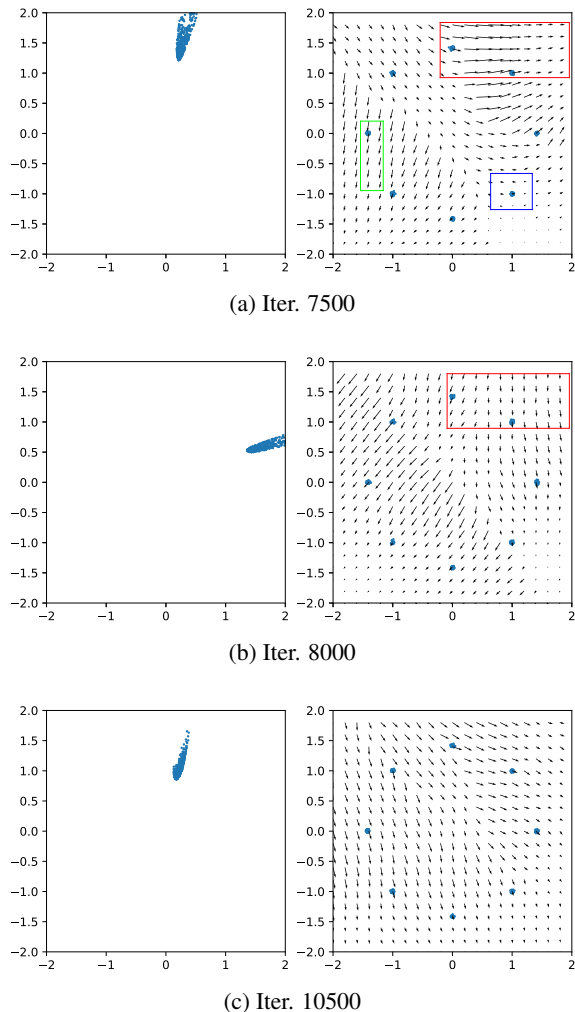


Figure 1. Catastrophic forgetting in GAN on a toy dataset of 8 Gaussian distributions. D uses the original GAN loss (Goodfellow et al., 2014). The discriminator and generator are MLPs with randomly initialized weights, plain stochastic gradient descent (SGD) is used for optimization, large mini-batches are used to ensure that a mini-batch contains real samples from all modes. On the left are samples from generator’s distributions at different training iterations. On the right are the gradient $-\frac{\partial \mathcal{L}_D}{\partial \mathbf{x}}$ for different values of \mathbf{x} at different training iterations. For each point \mathbf{x} , the vector shows the direction and the length the point should move in order to decrease the loss \mathcal{L}_D . Because G learns to fool D , it should move fake samples in the directions of the corresponding vectors. When fake samples move (or the model distribution changes), the directions of a large number of vectors also change (red boxes). These vectors do not point toward the closest real sample but toward directions that move the corresponding points away from fake samples. D assigns high scores to points further away from fake samples, regardless of the true label of each point. It suggests that D focuses its capacity on discriminating the current model distribution from the nearby part of target distribution. D , therefore, cannot effectively teach G to approximate the entire target distribution p_r . Because D has forgot about past model distributions, G can turn back to its old states to fool D and form a learning loop. In our experiment, fake samples rotate around the big circle for many cycles. The discriminator and generator at iteration 10500 are very similar to what they were 3000 iterations ago.

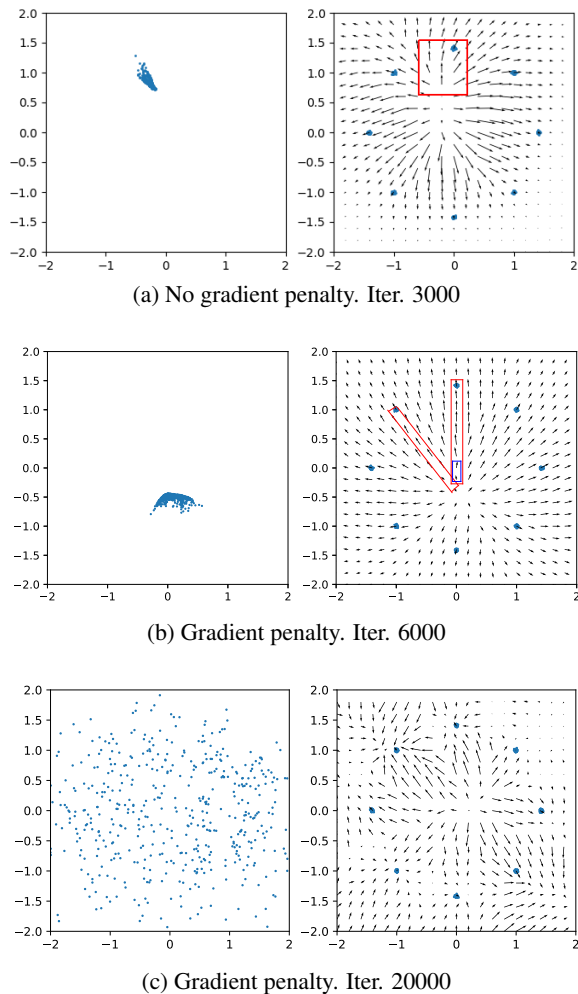


Figure 2. The effect of gradient penalty with $k = 0$ in preventing catastrophic forgetting and mode collapse. G and D are MLPs, plain SGD is used for optimization. (a) Fake samples are concentrated in a small regions of the space and are attracted toward the same real sample (or a small number of real samples). As the training continues, mode collapse happens. (b) Gradients along the line segment connecting a fake and a real sample have large norm and point toward the real sample (red boxes). Note that a vector in the blue box do not point toward the closest real sample but to the real sample the fake sample is paired with. Although fake samples are concentrated in a small region, they are attracted towards different real samples. (c) As the training progresses, fake samples are spread out over the space, eliminating the risk of mode collapse.

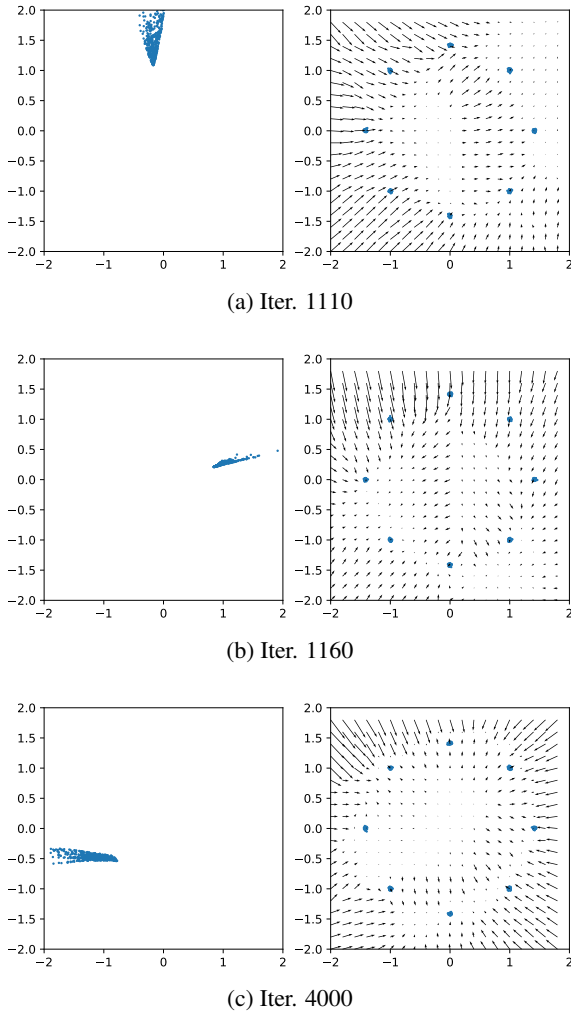


Figure 3. The effect of momentum based optimizers in preventing catastrophic forgetting. SGD is replaced by ADAM (Kingma & Ba, 2014). When fake samples move from one mode to another, the directions and scales of the gradient vectors remain stable. The majority of vectors point toward the closest real samples. It shows that D does not focus as much on achieving high classification accuracy on current mini-batch.

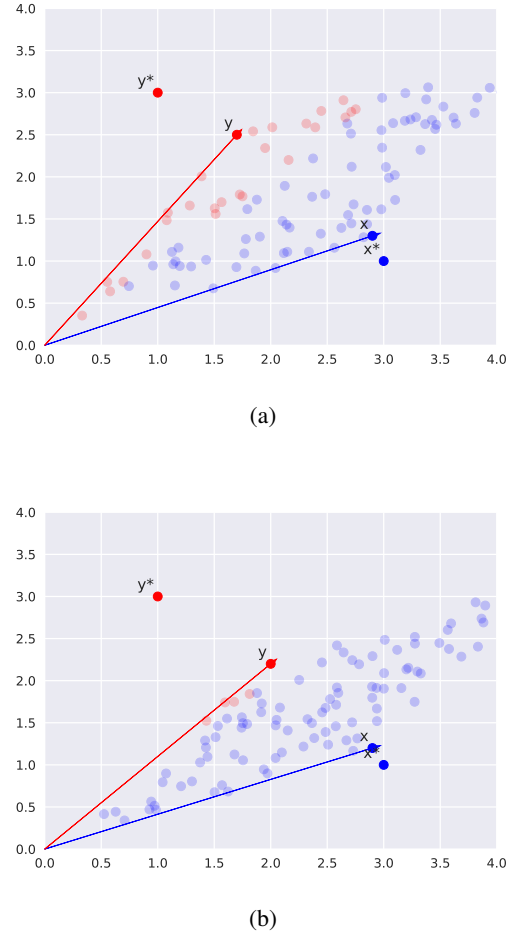


Figure 4. (a) Each point in light color represents an output $\tilde{x} = W\mathbf{a}$. Data point closer to \mathbf{x}^* are shown in light blue, data points closer to \mathbf{y}^* are shown in light red. For random input activation $\mathbf{a} \succeq \mathbf{0}$, the probability that \tilde{x} is closer to \mathbf{x}^* is higher than the probability that \tilde{x} is closer to \mathbf{y}^* . (b) SGD moves \mathbf{x} and \mathbf{y} closer to \mathbf{x}^* . When \mathbf{y} is closer to \mathbf{x}^* , the probability that the output \tilde{x} is closer to \mathbf{x}^* increases. Although \mathbf{y} is still closer to \mathbf{y}^* than to \mathbf{x}^* , the vast majority of the outputs are in the basin of attraction of \mathbf{x}^* .

4. Conclusion

In this paper, we discuss the cause and the dynamic of catastrophic forgetting and mode collapse in GAN. We show the relationship between catastrophic forgetting and mode collapse, and study existing solutions for these problems. We show that gradient penalties help the discriminator to distribute its capacity over the space, and momentum based optimizers help the discriminator to distribute its capacity over time. Together, they help to prevent catastrophic forgetting and mode collapse in GAN.

5. Future works

5.1. Memorizing gradient information with neural networks

In 2.2, we show that the running average of the gradient is a simple memory that helps the network to remember gradient information for longer time period. A natural extension to this simple memory is to use a neural network to store gradient information. Andrychowicz et al. (2016) used a LSTM (Hochreiter & Schmidhuber, 1997) to compute the update for parameter of the main network. The method outperformed hand designed optimizers such as ADAM (Kingma & Ba, 2014). Therefore, using neural network based optimizers could improve the stability of GAN.

5.2. Online EWC for GAN

In section 2, we formulate the training of GAN as a sequential learning problem and show that catastrophic forgetting damages GAN's performance. Method such as EWC (Kirkpatrick et al., 2017) are proven to be effective in preventing catastrophic forgetting. However, the Fisher information matrix which encodes the importance of each parameter must be computed at the end of each task. If we consider each training step of GAN a task, then naive application of EWC to GAN would be prohibitively expensive as the Fisher information matrix need to be computed at every training step. Zenke et al. (2017) proposed to compute the importance for each parameter online using first order gradient information. Therefore, the algorithm is more suitable to the context of GAN. We plan to perform experiments to verify the effectiveness of this algorithm.

References

Andrychowicz, Marcin, Denil, Misha, Gómez, Sergio, Hoffman, Matthew W, Pfau, David, Schaul, Tom, and de Freitas, Nando. Learning to learn by gradient descent by gradient descent. In Lee, D. D., Sugiyama, M., Luxburg, U. V., Guyon, I., and Garnett, R. (eds.), *Advances in Neural Information Processing Systems 29*, pp. 3981–3989. Curran Associates, Inc.,

2016. URL <http://papers.nips.cc/paper/6461-learning-to-learn-by-gradient-descent-by-gradient-descent.pdf>.

Arjovsky, Martin, Chintala, Soumith, and Bottou, Léon. Wasserstein generative adversarial networks. In Precup, Doina and Teh, Yee Whye (eds.), *Proceedings of the 34th International Conference on Machine Learning*, volume 70 of *Proceedings of Machine Learning Research*, pp. 214–223, International Convention Centre, Sydney, Australia, 06–11 Aug 2017. PMLR.

Arora, Sanjeev, Ge, Rong, Liang, Yingyu, Ma, Tengyu, and Zhang, Yi. Generalization and equilibrium in generative adversarial nets (GANs). In Precup, Doina and Teh, Yee Whye (eds.), *Proceedings of the 34th International Conference on Machine Learning*, volume 70 of *Proceedings of Machine Learning Research*, pp. 224–232, International Convention Centre, Sydney, Australia, 06–11 Aug 2017. PMLR.

Fedus, William, Rosca, Mihaela, Lakshminarayanan, Balaji, Dai, Andrew M., Mohamed, Shakir, and Goodfellow, Ian. Many paths to equilibrium: GANs do not need to decrease a divergence at every step. In *International Conference on Learning Representations*, 2018. URL <https://openreview.net/forum?id=ByQpn1ZA->.

French, Robert M. Catastrophic forgetting in connectionist networks. *Trends in Cognitive Sciences*, 3(4):128 – 135, 1999. ISSN 1364-6613. doi: [https://doi.org/10.1016/S1364-6613\(99\)01294-2](https://doi.org/10.1016/S1364-6613(99)01294-2). URL <http://www.sciencedirect.com/science/article/pii/S1364661399012942>.

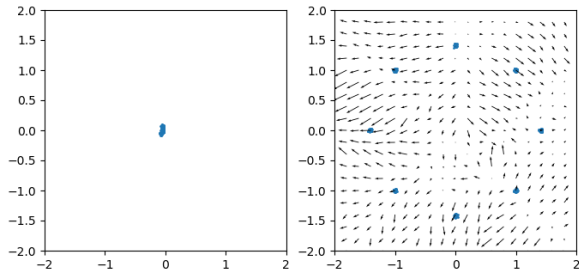
Fukushima, Kunihiko. Neocognitron: A self-organizing neural network model for a mechanism of pattern recognition unaffected by shift in position. *Biological Cybernetics*, 36(4):193–202, Apr 1980. ISSN 1432-0770. doi: 10.1007/BF00344251. URL <https://doi.org/10.1007/BF00344251>.

Goodfellow, Ian, Pouget-Abadie, Jean, Mirza, Mehdi, Xu, Bing, Warde-Farley, David, Ozair, Sherjil, Courville, Aaron, and Bengio, Yoshua. Generative adversarial nets. In Ghahramani, Z., Welling, M., Cortes, C., Lawrence, N. D., and Weinberger, K. Q. (eds.), *Advances in Neural Information Processing Systems 27*, pp. 2672–2680. Curran Associates, Inc., 2014. URL <http://papers.nips.cc/paper/5423-generative-adversarial-nets.pdf>.

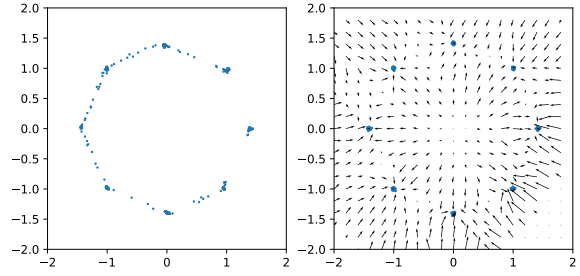
Gulrajani, Ishaan, Ahmed, Faruk, Arjovsky, Martin, Dumoulin, Vincent, and Courville, Aaron C. Improved training of wasserstein gans. In Guyon, I., Luxburg, U. V., Bengio, S., Wallach, H., Fergus, R., Vishwanathan, S., and Garnett, R. (eds.), *Advances*

- in *Neural Information Processing Systems 30*, pp. 5767–5777. Curran Associates, Inc., 2017. URL <http://papers.nips.cc/paper/7159-improved-training-of-wasserstein-gans.pdf>.
- Hochreiter, Sepp and Schmidhuber, Jürgen. Long short-term memory. *Neural Comput.*, 9(8):1735–1780, November 1997. ISSN 0899-7667. doi: 10.1162/neco.1997.9.8.1735. URL <http://dx.doi.org/10.1162/neco.1997.9.8.1735>.
- Ioffe, Sergey and Szegedy, Christian. Batch normalization: Accelerating deep network training by reducing internal covariate shift. In Bach, Francis and Blei, David (eds.), *Proceedings of the 32nd International Conference on Machine Learning*, volume 37 of *Proceedings of Machine Learning Research*, pp. 448–456, Lille, France, 07–09 Jul 2015. PMLR. URL <http://proceedings.mlr.press/v37/ioffe15.html>.
- Kingma, Diederik P. and Ba, Jimmy. Adam: A method for stochastic optimization. *CoRR*, abs/1412.6980, 2014. URL <http://arxiv.org/abs/1412.6980>.
- Kirkpatrick, James, Pascanu, Razvan, Rabinowitz, Neil, Veness, Joel, Desjardins, Guillaume, Rusu, Andrei A., Milan, Kieran, Quan, John, Ramalho, Tiago, Grabska-Barwinska, Agnieszka, Hassabis, Demis, Clopath, Claudia, Kumaran, Dharshan, and Hadsell, Raia. Overcoming catastrophic forgetting in neural networks. *Proceedings of the National Academy of Sciences*, 114(13):3521–3526, 2017. ISSN 0027-8424. doi: 10.1073/pnas.1611835114. URL <http://www.pnas.org/content/114/13/3521>.
- Kodali, Naveen, Abernethy, Jacob D., Hays, James, and Kira, Zsolt. On convergence and stability of gans. *CoRR*, abs/1705.07215, 2017. URL <http://arxiv.org/abs/1705.07215>.
- LeCun, Yann, Bottou, Léon, Bengio, Yoshua, and Haffner, Patrick. Gradient-based learning applied to document recognition. *Proceedings of the IEEE*, 86(11):2278–2324, 1998.
- Qian, Ning. On the momentum term in gradient descent learning algorithms. *Neural Networks*, 12(1):145 – 151, 1999. ISSN 0893-6080. doi: [https://doi.org/10.1016/S0893-6080\(98\)00116-6](https://doi.org/10.1016/S0893-6080(98)00116-6). URL <http://www.sciencedirect.com/science/article/pii/S0893608098001166>.
- Radford, Alec, Metz, Luke, and Chintala, Soumith. Unsupervised representation learning with deep convolutional generative adversarial networks. *CoRR*, abs/1511.06434, 2015. URL <http://arxiv.org/abs/1511.06434>.
- Seff, Ari, Beatson, Alex, Suo, Daniel, and Liu, Han. Continual learning in generative adversarial nets. *CoRR*, abs/1705.08395, 2017. URL <http://arxiv.org/abs/1705.08395>.
- Shin, Hanul, Lee, Jung Kwon, Kim, Jaehong, and Kim, Jiwon. Continual learning with deep generative replay. In Guyon, I., Luxburg, U. V., Bengio, S., Wallach, H., Fergus, R., Vishwanathan, S., and Garnett, R. (eds.), *Advances in Neural Information Processing Systems 30*, pp. 2990–2999. Curran Associates, Inc., 2017. URL <http://papers.nips.cc/paper/6892-continual-learning-with-deep-generative-replay.pdf>.
- Zenke, Friedemann, Poole, Ben, and Ganguli, Surya. Continual learning through synaptic intelligence. In Precup, Doina and Teh, Yee Whye (eds.), *Proceedings of the 34th International Conference on Machine Learning*, volume 70 of *Proceedings of Machine Learning Research*, pp. 3987–3995, International Convention Centre, Sydney, Australia, 06–11 Aug 2017. PMLR. URL <http://proceedings.mlr.press/v70/zenke17a.html>.

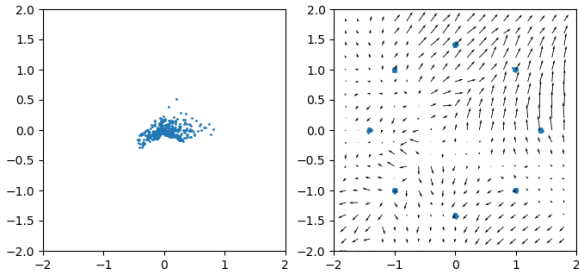
A. GAN trained with different settings



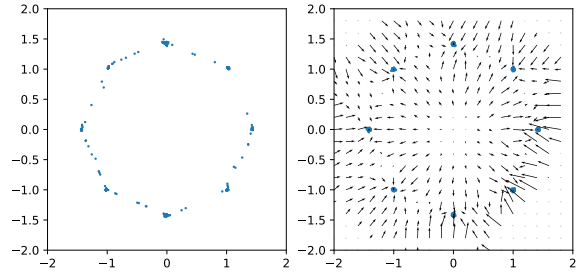
(a) No batch normalization. Iter. 0



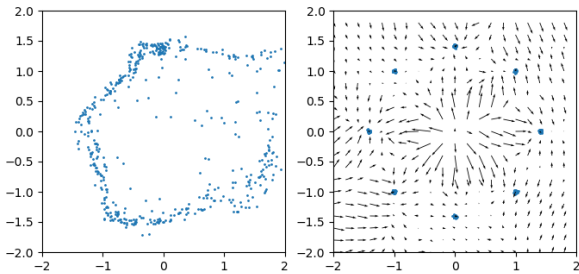
(a) Iter. 6000



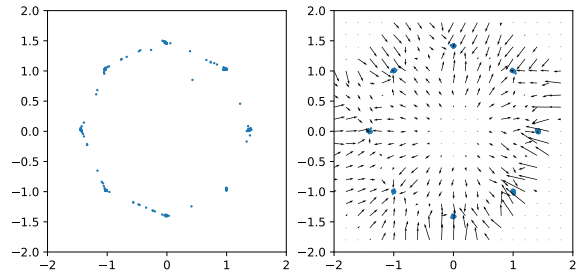
(b) Batch normalization. Iter. 0



(b) Iter. 10000



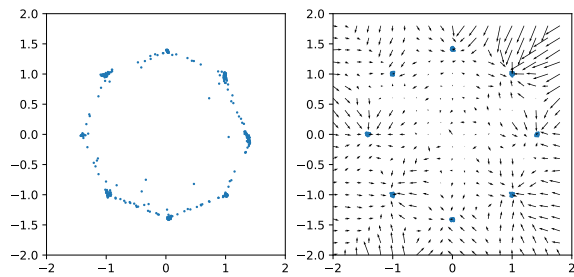
(c) Batch normalization. Iter. 11000



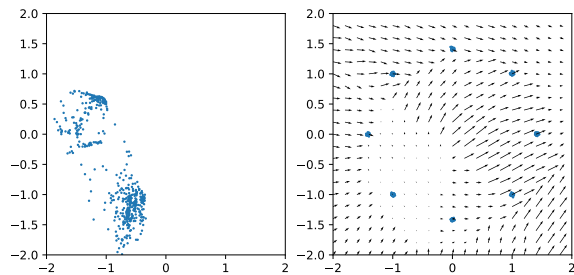
(c) Iter. 14000

Figure 5. The effect of batch normalization in preventing mode collapse. SGD optimizer was used in the experiment. Batch normalization spread fake samples over the space so they fall in the basin of attraction of different real samples.

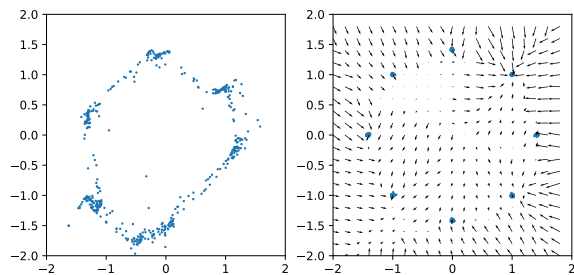
Figure 6. GAN trained with ADAM and batch normalization, no gradient penalty was used. As the training continues, the gradient patterns stay the unchanged, signifying that the training has converged.



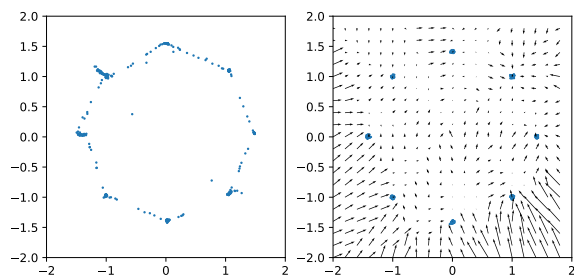
(a) Iter. 6000



(b) Iter. 7200



(c) Iter. 8000



(d) Iter. 14000

Figure 7. GAN trained with ADAM and gradient penalty as proposed in Gulrajani et al. (2017). Although the generator can already well approximate the target distribution at iteration 6000, the gradient penalty continues to push fake samples toward random real samples. The generator and discriminator oscillate around the equilibrium and do not converge. Note the difference between the gradient patterns in this experiment with the experiment in Fig. 6